

*Journal of*  
***Mechanics of  
Materials and Structures***

**THE DETERMINATION OF FREQUENCIES OF  
LAMINATED CONICAL SHELLS VIA THE DISCRETE  
SINGULAR CONVOLUTION METHOD**

Ömer Civalek

***Volume 1, N° 1***

***January 2006***



mathematical sciences publishers



## THE DETERMINATION OF FREQUENCIES OF LAMINATED CONICAL SHELLS VIA THE DISCRETE SINGULAR CONVOLUTION METHOD

ÖMER CIVALEK

The discrete singular convolution (DSC) algorithm for determining the frequencies of the free vibration of laminated conical shells is developed by using a numerical solution of the governing differential equations of motion based on Love's first approximation thin shell theory. By applying the discrete singular convolution method, the free vibration equations of motion of the composite laminated conical shell are transformed to a set of algebraic equations. Convergence and comparison studies are carried out to check the validity and accuracy of the DSC method.

### 1. Introduction

Because of the practical importance of the free vibration analysis of the composite laminated conical shell in structural, aerospace, nuclear, petrochemical, submarine hulls, and mechanical applications, a few investigators have made efforts to deal with free vibration analysis of this type of structures. Unsymmetric free vibrations of orthotropic sandwich shells of revolution has been made by Bacon and Bert [1967]. Siu and Bert [1970] analyzed the free vibration of isotropic and orthotropic conical shells by using the Rayleigh–Ritz technique. Irie et al. [1982; 1984] developed a transfer-matrix approach for free vibration of conical shells with constant and variable thickness. Using the finite element method, Sivadas and Ganesan [1992] analyzed the free vibration of conical shells with uniform thickness. Yang [1974] adopted the integration method in the vibration analysis of orthotropic conical shells. Tong [1993b; 1993a], and Tong and Wang [1992] examined the vibration and buckling analysis of isotropic, orthotropic and laminated conical shells by the power series expansion method. More recent papers [Shu 1996b; 1996a; Hua 2000; Hua and Lam 2000; Lam and Hua 1997] have used the differential quadrature method to study the free vibration of orthotropic and laminated rotating conical shells. Liew et al. [1995] also studied the effects of initial twist and thickness variation on the vibration behavior of shallow conical shells. Lim and Kitipornchai [1999] have investigated the effects of subtended and

---

*Keywords:* conical shells, discrete singular convolution, laminated composite, frequencies.

vertex angles on the free vibration of open conical shell. Some selected works in this topic includes [Liew et al. 2005; Liew and Lim 1994; Lim et al. 1997; 1998; Lim and Liew 1995; Leissa 1973; Soedel 1996; Civalek 1998; 2004; 2005; Civalek and Ülker 2005]. More detailed information can be found in [Chang 1981] and [Kapania 1989].

The focus in this work is on the application of the DSC method to the differential equation, which governs the free vibration analysis of laminated conical shells. The governing differential equations of vibration of the shell are formulated using Love's first approximation classical thin shell theory [Love 1888]. In this study, the DSC method was used for spatial discretization of the differential equations governing the problem. In the author's knowledge, it is the first time the discrete singular convolution algorithm has been successfully applied to laminated conical shell problem for vibration analysis.

## 2. Governing equations

A typical laminated conical shell is given as shown in Figure 1. The cone semiver-  
tex angle, thickness of the shell, and cone length are denoted by  $\alpha$ ,  $h$  and  $L$ .  $R_1$  and  $R_2$  are the radii of the cone at its small and large edges. The conical shell is

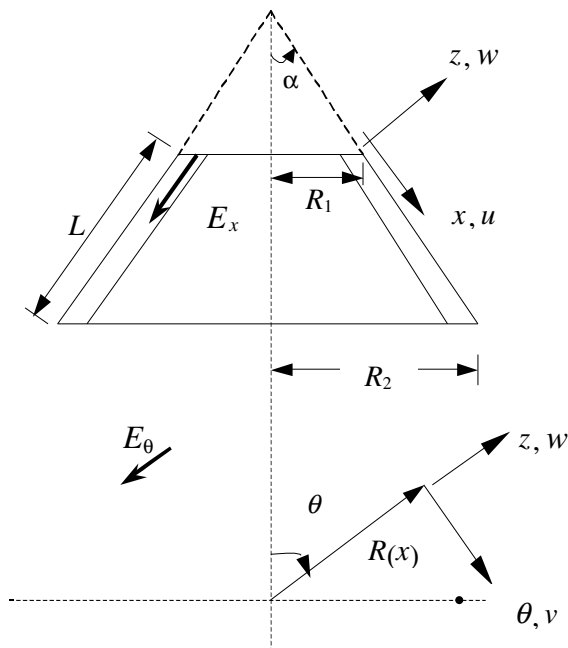


**Figure 1.** Geometry and notation of laminated conical shell.

referred to a coordinate system  $(x, \theta, z)$  as shown in Figure 1. The components of the deformation of the conical shell with references to this given coordinate system are denoted by  $u, v, w$  in the  $x, \theta$  and  $z$  directions, respectively.  $E_x$  and  $E_\theta$  denote the elastic moduli respectively in the meridional  $x$  and circumferential  $\theta$  directons. The equilibrium equation of motion in terms of the force and moment resultants can be written as in [Tong 1993b]:

$$\frac{\partial N_x}{\partial x} + \frac{1}{R(x)} \frac{\partial N_{x\theta}}{\partial \theta} + \frac{\sin \alpha}{R(x)} (N_x - N_\theta) = \rho h \frac{\partial^2 u}{\partial t^2}, \quad (1)$$

$$\frac{\partial N_{x\theta}}{\partial x} + \frac{1}{R(x)} \frac{\partial N_\theta}{\partial \theta} + \frac{\cos \alpha}{R(x)} \frac{\partial M_{x\theta}}{\partial x} + \frac{\cos^2 \alpha}{R^2(x)} \frac{\partial M_\theta}{\partial \theta} + 2 \frac{\sin \alpha}{R(x)} N_{x\theta} = \rho h \frac{\partial^2 v}{\partial t^2}, \quad (2)$$

$$\begin{aligned} \frac{\partial^2 M_x}{\partial x^2} + \frac{2}{R(x)} \frac{\partial^2 M_{x\theta}}{\partial \theta \partial x} + \frac{1}{R^2(x)} \frac{\partial^2 M_\theta}{\partial \theta^2} + \frac{2 \sin \alpha}{R(x)} \frac{\partial M_x}{\partial x} \\ - \frac{1}{R(x)} \left( \sin \alpha \frac{\partial M_\theta}{\partial x} + \cos \alpha N_\theta \right) = \rho h \frac{\partial^2 w}{\partial t^2}, \end{aligned} \quad (3)$$

where

$$R(x) = R_1 + x \sin \alpha, \quad (4)$$

$$\rho_a(x, \theta) = \frac{1}{h} \int_{-h/2}^{h/2} \rho(x, \theta, z) dz. \quad (5)$$

Here  $\rho$  is the density and  $\rho_a$  the linear density. The moment resultants and in-surface force are

$$N = (N_x, N_\theta, N_{x\theta})^T = \int_{-h/2}^{h/2} (\sigma_x, \sigma_\theta, \sigma_{x\theta})^T dz, \quad (6)$$

$$M = (M_x, M_\theta, M_{x\theta})^T = \int_{-h/2}^{h/2} (\sigma_x, \sigma_\theta, \sigma_{x\theta})^T z dz, \quad (7)$$

where  $(\sigma)^T = \{\sigma_x, \sigma_\theta, \sigma_{x\theta}\}$  is the stress vector. The stress vector of the  $k$ -th layer for laminated composite conical shells in which each layer is orthotropic is

$$\{\sigma_k\} = [Q_{ij}^*] \{\varepsilon_k^*\}, \quad (8)$$

where  $\{\varepsilon_k^*\}^T = \{\varepsilon_x, \varepsilon_\theta, \varepsilon_{x\theta}\}$  is the strain vector. Based on Love's first approximation theory, the strain components of this vector are defined as linear functions of the normal (thickness) coordinate  $z$ :

$$\varepsilon_x = \varepsilon_1 + z\kappa_1, \quad \varepsilon_\theta = \varepsilon_2 + z\kappa_2, \quad \varepsilon_{x\theta} = \gamma + 2z\tau \quad (9)$$

where  $\{\varepsilon\}^T = \{\varepsilon_1, \varepsilon_2, \gamma\}$  and  $\{\kappa\}^T = \{\kappa_1, \kappa_2, 2\tau\}$  are the strain and curvature vectors of the reference surface. They are defined by

$$\begin{aligned}\varepsilon_1 &= \frac{\partial u}{\partial x}, & \varepsilon_2 &= \frac{1}{R(x)} \frac{\partial v}{\partial \theta} + \frac{u \sin \alpha}{R(x)} + \frac{w \cos \alpha}{R(x)}, & \gamma &= \frac{1}{R(x)} \frac{\partial u}{\partial \theta} + \frac{\partial v}{\partial x} - \frac{v \sin \alpha}{R(x)} \\ \kappa_1 &= -\frac{\partial^2 w}{\partial x^2}, & \kappa_2 &= -\frac{1}{R^2(x)} \frac{\partial^2 w}{\partial \theta^2} + \frac{\cos \alpha}{R^2(x)} \frac{\partial v}{\partial \theta} - \frac{\sin \alpha}{R(x)} \frac{\partial w}{\partial x}, \\ \tau &= -\frac{1}{R(x)} \frac{\partial^2 w}{\partial x \partial \theta} + \frac{\sin \alpha}{R^2(x)} \frac{\partial w}{\partial \theta} + \frac{\cos \alpha}{R(x)} \frac{\partial v}{\partial x} - \frac{v \sin \alpha \cos \alpha}{R^2(x)}.\end{aligned}\quad (10)$$

For a thin and generally orthotropic layer, the stresses defined in Equation (8) are given by

$$\begin{Bmatrix} \sigma_x \\ \sigma_\theta \\ \sigma_{x\theta} \end{Bmatrix} = \begin{bmatrix} Q_{11}^* & Q_{12}^* & Q_{16}^* \\ Q_{12}^* & Q_{22}^* & Q_{26}^* \\ Q_{16}^* & Q_{26}^* & Q_{66}^* \end{bmatrix} \begin{Bmatrix} \varepsilon_x \\ \varepsilon_\theta \\ \varepsilon_{\theta x} \end{Bmatrix}, \quad (11)$$

where the transformed reduced stiffness matrix of the  $k$ -th layer is defined by

$$[Q_k^*] = [T][Q_k][T]^{-1} \quad (12)$$

and where

$$[T] = \begin{bmatrix} \cos^2 \varphi & \sin^2 \varphi & 2 \sin \varphi \cos \varphi \\ \sin^2 \varphi & \cos^2 \varphi & -2 \sin \varphi \cos \varphi \\ -\sin \varphi \cos \varphi & \sin \varphi \cos \varphi & \cos^2 \varphi - \sin^2 \varphi \end{bmatrix} \quad (13)$$

in which  $[T]$  is the transformation matrix between the material principal coordinate of the  $k$ -th layer and the geometric coordinate of the laminated composite conical shell;  $\varphi$  is the angle between these two coordinate directions. The force and moment resultants are given in terms of displacements  $u$ ,  $v$  and  $w$  by

$$\begin{Bmatrix} N_x \\ N_\theta \\ N_{x\theta} \\ M_x \\ M_\theta \\ M_{x\theta} \end{Bmatrix} = \begin{bmatrix} c_{11} & c_{12} & c_{13} \\ c_{21} & c_{22} & c_{23} \\ c_{31} & c_{32} & c_{33} \\ c_{41} & c_{42} & c_{43} \\ c_{51} & c_{52} & c_{53} \\ c_{61} & c_{62} & c_{63} \end{bmatrix} \begin{Bmatrix} u \\ v \\ w \end{Bmatrix}, \quad (14)$$

where

$$\begin{aligned}
 c_{i1} &= A_{i1} \frac{\partial}{\partial x} + A_{i2} \frac{\sin \alpha}{R(x)}, & c_{i2} &= \frac{A_{i2}}{R(x)} \frac{\partial}{\partial \theta}, \\
 c_{i3} &= -A_{i2} \frac{\cos \alpha}{R(x)} - B_{1i} \frac{\partial^2}{\partial x^2} - B_{i2} \frac{\sin \alpha}{R(x)} \frac{\partial}{\partial x} - \frac{B_{i2}}{R^2(x)} \frac{\partial^2}{\partial \theta^2}, \\
 c_{31} &= \frac{A_{66}}{R(x)} \frac{\partial}{\partial \theta}, & c_{32} &= A_{66} \left( \frac{\partial}{\partial x} - \frac{\sin \alpha}{R(x)} \right), & c_{33} &= -B_{66} \frac{\partial}{\partial x} \left( \frac{1}{R(x)} \frac{\partial}{\partial \theta} \right) \\
 c_{ji} &= B_{1i} \frac{\partial}{\partial x} + \frac{B_{i2} \sin \alpha}{R(x)}, & c_{j2} &= \frac{B_{i2}}{R(x)} \frac{\partial}{\partial \theta}, \\
 c_{j3} &= -D_{1i} \frac{\partial^2}{\partial x^2} - D_{i2} \frac{\sin \alpha}{R(x)} \frac{\partial}{\partial x} - \frac{D_{i2}}{R^2(x)} \frac{\partial^2}{\partial \theta^2} - B_{i2} \frac{\cos \alpha}{R(x)}, \\
 c_{61} &= \frac{B_{66}}{R(x)} \frac{\partial}{\partial \theta}, & c_{62} &= B_{66} \left( \frac{\partial}{\partial x} - \frac{\sin \alpha}{R(x)} \right), & c_{63} &= -2D_{66} \frac{\partial}{\partial x} \left( \frac{1}{R(x)} \frac{\partial}{\partial \theta} \right).
 \end{aligned} \tag{15}$$

Here  $i = 1, 2$  and  $j = 3 + i$ . the tensors  $A_{ij}$ ,  $B_{ij}$  and  $D_{ij}$  represent the extensional, coupling and bending stiffnesses and are calculated from the equations

$$(A_{ij}, B_{ij}, D_{ij}) = \int_{-h/2}^{h/2} Q_{ij}^*(1, z, z^2) dz. \tag{16}$$

For an arbitrarily laminated composite shell, these stiffnesses can be given as

$$\begin{aligned}
 (A_{ij}) &= \sum_{k=1}^{N_L} Q_{ij}^{(k)} (h_k - h_{k-1}), & (B_{ij}) &= \frac{1}{2} \sum_{k=1}^{N_L} Q_{ij}^{(k)} (h_k^2 - h_{k-1}^2), \\
 (D_{ij}) &= \frac{1}{3} \sum_{k=1}^{N_L} Q_{ij}^{(k)} (h_k^3 - h_{k-1}^3),
 \end{aligned} \tag{17}$$

where  $N_L$  is the number of total layers of the laminated conical shell,  $Q_{ij}^{(k)}$  is the element of the transformed reduced stiffness matrix for the  $k$ -th layer, and  $h_k$  and  $h_{k-1}$  denote distances from the shell reference surface to the outer and inner surfaces of the  $k$ -th layer. Substituting Equation (14) into Equations (1)–(3), we obtain the governing equations for the linear free vibration analysis of composite laminated conical shells:

$$L_{11}u + L_{12}v + L_{13}w = \rho h \frac{\partial^2 u}{\partial t^2}, \tag{18a}$$

$$L_{21}u + L_{22}v + L_{23}w = \rho h \frac{\partial^2 v}{\partial t^2}, \tag{18b}$$

$$L_{31}u + L_{32}v + L_{33}w = \rho h \frac{\partial^2 w}{\partial t^2}, \tag{18c}$$

where

$$L_{11} = A_{11} \frac{\partial^2}{\partial x^2} + A_{11} \frac{\sin \alpha}{R(x)} \frac{\partial}{\partial x} - A_{22} \frac{\sin^2 \alpha}{R^2(x)} + \frac{A_{66}}{R^2(x)} \frac{\partial^2}{\partial \theta^2}, \quad (19)$$

$$L_{12} = \frac{(A_{12} + A_{66})}{R(x)} \frac{\partial^2}{\partial x \partial \theta} - \frac{(A_{22} + A_{66}) \sin \alpha}{R^2(x)} \frac{\partial}{\partial \theta} + \frac{(B_{12} + 2B_{66}) \cos \alpha}{R^2(x)} \frac{\partial^2}{\partial x \partial \theta} + \frac{(B_{12} + B_{22} + 2B_{66}) \sin \alpha \cos \alpha}{R(x)} \frac{\partial}{\partial \theta}, \quad (20)$$

$$L_{13} = A_{12} \frac{\cos \alpha}{R(x)} \frac{\partial}{\partial x} - A_{22} \frac{\sin \alpha \cos \alpha}{R^2(x)} - B_{11} \frac{\partial^3}{\partial x^3} - \frac{(B_{12} + 2B_{66}) \cos \alpha}{R^2(x)} \frac{\partial^3}{\partial x \partial \theta^2} - B_{11} \frac{\sin \alpha}{R(x)} \frac{\partial^2}{\partial x^2} + \frac{(B_{12} + B_{22} + 2B_{66}) \sin \alpha}{R^2(x)} \frac{\partial^2}{\partial \theta^2} + B_{22} \frac{\sin^2 \alpha}{R^2(x)} \frac{\partial}{\partial x}, \quad (21)$$

$$L_{21} = \frac{(A_{12} + A_{66})}{R(x)} \frac{\partial^2}{\partial x \partial \theta} + \frac{(A_{22} + A_{66}) \sin \alpha}{R^2(x)} \frac{\partial}{\partial \theta} + \frac{(B_{12} + B_{66}) \cos \alpha}{R^2(x)} \frac{\partial^2}{\partial x \partial \theta} + \frac{(B_{22} - B_{66}) \sin \alpha \cos \alpha}{R^3(x)} \frac{\partial}{\partial \theta}, \quad (22)$$

$$L_{22} = A_{66} \left( \frac{\partial^2}{\partial x^2} + \frac{\sin \alpha}{R(x)} \frac{\partial}{\partial x} - \frac{\sin^2 \alpha}{R^2(x)} \right) + \left( \frac{A_{22}}{R^2(x)} + 2B_{22} \frac{\cos \alpha}{R^3(x)} + \frac{D_{22} \cos^2 \alpha}{R^4(x)} \right) \frac{\partial^2}{\partial \theta^2} + 2 \frac{D_{66} \cos^2 \alpha}{R^2(x)} \left( \frac{\partial^2}{\partial x^2} - \frac{2 \sin \alpha}{R(x)} \frac{\partial}{\partial x} + \frac{2 \sin^2 \alpha}{R^2(x)} \right) + \frac{B_{66} \cos \alpha}{R(x)} \left( 3 \frac{\partial^2}{\partial x^2} - \frac{\sin \alpha}{R(x)} \frac{\partial}{\partial x} + \frac{\sin^2 \alpha}{R^2(x)} \right), \quad (23)$$

$$L_{23} = \left( \frac{A_{22} \cos \alpha}{R^2(x)} + \frac{B_{22} \cos \alpha}{R^3(x)} - \frac{4D_{66} \cos \alpha \sin^2 \alpha}{R^4(x)} \right) \frac{\partial}{\partial \theta} - \left( \frac{B_{22}}{R^3(x)} + \frac{D_{22} \cos \alpha}{R^4(x)} \right) \frac{\partial^3}{\partial \theta^3} - \left( \frac{B_{22}}{R^2(x)} + \frac{(D_{22} - 4D_{66}) \sin \alpha \cos \alpha}{R^3(x)} \right) \frac{\partial^2}{\partial x \partial \theta} - \left( \frac{(B_{12} + 2B_{66})}{R(x)} + \frac{(D_{12} + 2D_{66}) \cos \alpha}{R^2(x)} \right) \frac{\partial^3}{\partial x^2 \partial \theta}, \quad (24)$$

$$L_{31} = -A_{12} \frac{\cos \alpha}{R(x)} \frac{\partial}{\partial x} - A_{22} \frac{\sin \alpha \cos \alpha}{R^2(x)} + B_{11} \frac{\partial^3}{\partial x^3} + \frac{(B_{12} + 2B_{66})}{R^2(x)} \frac{\partial^3}{\partial x \partial \theta^2} - \frac{2B_{11} \sin \alpha}{R(x)} \frac{\partial^2}{\partial x^2} + \frac{B_{22} \sin^2 \alpha}{R^2(x)} \frac{\partial}{\partial x} + \frac{(B_{22} - 2B_{66}) \sin \alpha}{R^3(x)} \frac{\partial^2}{\partial \theta^2} + \frac{B_{22} \sin^3 \alpha}{R^3(x)}, \quad (25)$$

$$\begin{aligned}
 L_{32} = & - \left( A_{22} \frac{\cos \alpha}{R^2(x)} - \frac{B_{22} \cos^2 \alpha - (B_{22} + 2B_{66}) \sin^2 \alpha}{R^3(x)} \right) \frac{\partial}{\partial \theta} \\
 & + \left( - \frac{(2D_{12} + 2D_{22} + 8D_{66}) \cos \alpha \sin^2 \alpha}{R^4(x)} \right) \frac{\partial}{\partial \theta} + \left( \frac{B_{22}}{R^3(x)} + \frac{D_{22} \cos \alpha}{R^4(x)} \right) \frac{\partial^3}{\partial \theta^3} \\
 & + \left( \frac{(B_{12} + 2B_{66})}{R(x)} + \frac{(D_{12} + 4D_{66}) \cos \alpha}{R^2(x)} \right) \frac{\partial^3}{\partial x^2 \partial \theta} \\
 & + \left( \frac{(B_{22} + 2B_{66}) \sin \alpha}{R^2(x)} + \frac{(D_{22} + 2D_{12} + 8D_{66}) \sin \alpha \cos \alpha}{R^3(x)} \right) \frac{\partial^2}{\partial x \partial \theta}, \quad (26)
 \end{aligned}$$

$$\begin{aligned}
 L_{33} = & -A_{22} \frac{\cos^2 \alpha}{R^2(x)} - \frac{2B_{12} \cos \alpha}{R(x)} \frac{\partial^2}{\partial x^2} + \frac{2B_{22} \cos \alpha}{R^3(x)} \frac{\partial^2}{\partial \theta^2} + \frac{B_{22} \cos \alpha \sin^2 \alpha}{R^3(x)} \\
 & + D_{11} \frac{\partial^4}{\partial x^4} - \frac{2(D_{12} + 2D_{66})}{R^2(x)} \frac{\partial^4}{\partial x^2 \partial \theta^2} - \frac{D_{22}}{R^4(x)} \frac{\partial^4}{\partial \theta^4} \\
 & - \frac{2D_{11} \sin \alpha}{R(x)} \frac{\partial^3}{\partial x^3} + \frac{2(D_{12} + 4D_{66}) \sin \alpha}{R^3(x)} \frac{\partial^3}{\partial x \partial \theta^2} + \frac{D_{22} \sin^2 \alpha}{R^2(x)} \frac{\partial^2}{\partial x^2} \\
 & - \frac{2(D_{12} + D_{22} + 4D_{66}) \sin^2 \alpha}{R^4(x)} \frac{\partial^2}{\partial \theta^2} - \frac{D_{22} \sin^3 \alpha}{R^3(x)} \frac{\partial}{\partial x}. \quad (27)
 \end{aligned}$$

The displacement terms are

$$\begin{aligned}
 u &= U(x) \cos(n\theta) \cos(\omega t), \quad v = V(x) \sin(n\theta) \cos(\omega t), \\
 w &= W(x) \cos(n\theta) \cos(\omega t). \quad (28)
 \end{aligned}$$

Substituting these equations into (18), we can write the governing equations as

$$\begin{aligned}
 G_{111}U + G_{112} \frac{\partial U}{\partial x} + G_{113} \frac{\partial^2 U}{\partial x^2} + G_{121}V + G_{122} \frac{\partial V}{\partial x} \\
 + G_{131}W + G_{132} \frac{\partial W}{\partial x} + G_{133} \frac{\partial^2 W}{\partial x^2} + G_{134} \frac{\partial^3 W}{\partial x^3} = -\rho h \omega^2 U, \quad (29)
 \end{aligned}$$

$$\begin{aligned}
 G_{211}U + G_{212} \frac{\partial U}{\partial x} + G_{221}V + G_{222} \frac{\partial V}{\partial x} + G_{223} \frac{\partial^2 V}{\partial x^2} \\
 + G_{231}W + G_{232} \frac{\partial W}{\partial x} = -\rho h \omega^2 V, \quad (30)
 \end{aligned}$$

$$\begin{aligned}
 G_{311}U + G_{312} \frac{\partial U}{\partial x} + G_{313} \frac{\partial^2 U}{\partial x^2} + G_{314} \frac{\partial^3 U}{\partial x^3} + G_{321}V + G_{322} \frac{\partial V}{\partial x} + G_{323} \frac{\partial^2 V}{\partial x^2} \\
 + G_{331}W + G_{332} \frac{\partial W}{\partial x} + G_{333} \frac{\partial^2 W}{\partial x^2} + G_{334} \frac{\partial^3 W}{\partial x^3} + G_{335} \frac{\partial^4 W}{\partial x^4} = -\rho h \omega^2 W, \quad (31)
 \end{aligned}$$

where  $G_{ijk}$  are the related coefficients, found in [Tong 1993b; Shu 1996b]. In this study, the following two type main boundary conditions are considered. These are defined as follows:

*Simply supported edge (S):*

$$V = 0, W = 0, N_x = 0, M_x = 0 \quad (32a)$$

*Clamped edge (C):*

$$U = 0, V = 0, W = 0 \text{ and } \partial W / \partial x = 0 \quad (32b)$$

### 3. Discrete singular convolution (DSC)

The discrete singular convolution (DSC) algorithm was introduced by Wei [1999]. He and coworkers [Wei 1999; 2001a; 2001b; Wei et al. 2002a; 2002b] first applied the DSC algorithm to solve solid and fluid mechanics problems. Zhao et al. [2002] analyzed the high frequency vibration of plates and plate vibration under irregular internal support using the DSC algorithm. Numerical solution of unsteady incompressible flows using DSC is given in [Wan et al. 2002]. More recently, Lim et al. [2005a; 2005b] presented the DSC–Ritz method for the free vibration analysis of Kirchhoff and Mindlin plates and thick shallow shells.

These studies indicates that the DSC algorithm work very well for the vibration analysis of plates, especially for high-frequency analysis of rectangular plates. It also suggests that the DSC algorithm has the accuracy of global methods and the flexibility of local methods for solving differential equations in applied mechanics. The mathematical foundation of the DSC algorithm is the theory of distributions and wavelet analysis. Consider a distribution  $T$  and let  $\eta(t)$  be an element of the space of test functions. A singular convolution can be defined by

$$F(t) = (T * \eta)(t) = \int_{-\infty}^{\infty} T(t-x)\eta(x) dx, \quad (33)$$

where  $T(t-x)$  is a singular kernel. The DSC algorithm can be realized using many approximation kernels. It has been shown that for many problems, the regularized Shannon kernel (RSK) is very efficient. This kernel is given by

$$\delta_{\Delta, \sigma}(x-x_k) = \frac{\sin((\pi/\Delta)(x-x_k))}{(\pi/\Delta)(x-x_k)} \exp\left(-\frac{(x-x_k)^2}{2\sigma^2}\right); \quad \sigma > 0 \quad (34)$$

(see [Wei 1999]), where  $\Delta = \pi/(N-1)$  is the grid spacing and  $N$  is the number of grid points. The parameter  $\sigma$  determines the width of the Gaussian envelope and often varies in association with the grid spacing, i.e.,  $\sigma = rh$ . Here  $r$  is a parameter chosen in computation. It is also known that the truncation error is very small due to the use of the Gaussian regularizer. The formulation in (34) is practical and has an

essentially compact support for numerical interpolation. With a sufficiently smooth approximation, it is more effective to consider a discrete singular convolution

$$F_\alpha(t) = \sum_k T_\alpha(t - x_k) f(x_k) \quad (35)$$

where  $F_\alpha(t)$  is an approximation to  $F(t)$  and  $\{x_k\}$  is an appropriate set of discrete points on which the DSC of (33) is well defined. Note that the original test function  $\eta(x)$  has been replaced by  $f(x)$ . This new discrete expression is suitable for computer realization. The mathematical property or requirement of  $f(x)$  is determined by the approximate kernel  $T_\alpha$ . In the DSC method, the function  $f(x)$  and its derivatives with respect to the  $x$  coordinate at a grid point  $x_i$  are approximated by a linear sum of discrete values  $f(x_k)$  in a narrow bandwidth  $[x - x_M, x + x_M]$ . This can be expressed as

$$\left. \frac{d^n f(x)}{dx^n} \right|_{x=x_i} = f^{(n)}(x) \approx \sum_{k=-M}^M \delta_{\Delta,\sigma}^{(n)}(x_i - x_k) f(x_k); \quad (n = 0, 1, 2, \dots), \quad (36)$$

where superscript  $n$  denotes the  $n$ -th derivative with respect to  $x$ . The  $x_k$  is a set of discrete sampling points centred around the point  $x$ ,  $\sigma$  is a regularization parameter,  $\Delta$  is the grid spacing, and  $2M + 1$  is the computational bandwidth, which is usually smaller than the size of the computational domain. The higher-order derivative terms  $\delta_{\Delta,\sigma}^{(n)}(x - x_k)$  in (34) are given by

$$\delta_{\Delta,\sigma}^{(n)}(x - x_k) = \left( \frac{d}{dx} \right)^n [\delta_{\Delta,\sigma}(x - x_k)], \quad (37)$$

where the differentiation can be carried out analytically. For example, the second derivative at  $x = x_i$  of the DSC kernel is

$$\delta_{\Delta,\sigma}^{(2)}(x - x_j) = \left. \frac{d^2}{dx^2} [\delta_{\Delta,\sigma}(x - x_j)] \right|_{x=x_i} \quad (38)$$

The discretized form of (6) can then be expressed as

$$f^{(2)}(x) = \left. \frac{d^2 f}{dx^2} \right|_{x=x_i} \approx \sum_{k=-M}^M \delta_{\Delta,\sigma}^{(2)}(k\Delta x_N) f_{i+k,j} \quad (39)$$

When the regularized Shannon's delta kernel (RSDK) is used, the detailed expressions for  $\delta_{\Delta,\sigma}(x)$ ,  $\delta_{\Delta,\sigma}^{(1)}(x)$ ,  $\delta_{\Delta,\sigma}^{(2)}(x)$ ,  $\delta_{\Delta,\sigma}^{(3)}(x)$  and  $\delta_{\Delta,\sigma}^{(4)}(x)$  can be easily obtained for  $x \neq x_k$ ; they are listed in the Appendix. Note that the differentiation matrix in (39) is in general banded. This is a great advantage in large scale computations. Consider a one dimensional,  $n$ -th order DSC kernel of delta type:

$$\delta_{\sigma,\Delta}^{(n)}(x - x_k), \quad n = 0, 1, 2, \dots \quad (40)$$

Here  $\delta_{\sigma,\Delta}^{(0)}(x - x_k) = \delta_{\sigma,\Delta}(x - x_k)$  is the DSC kernel of (36). These derivatives can be regarded as high pass filters. The filters corresponding to the derivatives of Shannon's kernel decay slowly as  $x$  increases, whereas the regularized filters are Schwarz class functions and have controlled residual amplitudes at large  $x$  values. In the Fourier representation, the derivatives of Shannon's kernel are discontinuous at certain points. In contrast, the derivatives of regularized kernels are all continuous and can be made very close to those of Shannon's if desired. The differential part of the operator on the coordinate grid is then represented by functional derivatives

$$D = \sum_{n=1} d_n(x) \frac{d^n}{dx^n} \rightarrow \sum_{n=1} d_n(x_m) \delta_{\alpha,\sigma}^{(n)}(x_m - x_k) \quad (41)$$

(see [Wei et al. 2002a]), where  $d_n(x)$  is a coefficient and  $\delta_{\alpha,\sigma}^{(n)}(x_m - x_k)$  is analytically given by

$$\delta_{\alpha,\sigma}^{(n)}(x_m - x_k) = \left( \frac{d}{dx} \right)^n \delta_{\alpha,\sigma}(x_m - x_k) \Big|_{x=x_m}. \quad (42)$$

Therefore, the discretized forms of Equations (29)–(31) can be expressed as

$$\begin{aligned} G_{111}U_{i,j} + G_{112} \sum_{k=-M}^M \delta_{\Delta,\sigma}^{(1)}(k\Delta x)U_{i+k,j} + G_{113} \sum_{k=-M}^M \delta_{\Delta,\sigma}^{(2)}(k\Delta x)U_{i+k,j} \\ + G_{121}V_{i,j} + G_{122} \sum_{k=-M}^M \delta_{\Delta,\sigma}^{(1)}(k\Delta x)V_{i,j+k} \\ + G_{131}W_{i,j} + G_{132} \sum_{k=-M}^M \delta_{\Delta,\sigma}^{(1)}(k\Delta x)W_{i,j+k} = -\rho h \omega^2 U_{i,j}, \quad (43a) \end{aligned}$$

$$\begin{aligned} G_{211}U_{i,j} + G_{212} \sum_{k=-M}^M \delta_{\Delta,\sigma}^{(1)}(k\Delta x)U_{i+k,j} \\ + G_{221}V_{i,j} + G_{222} \sum_{k=-M}^M \delta_{\Delta,\sigma}^{(1)}(k\Delta x)V_{i,j+k} + G_{223} \sum_{k=-M}^M \delta_{\Delta,\sigma}^{(2)}(k\Delta x)V_{i+k,j} \\ + G_{231}W_{i,j} + G_{232} \sum_{k=-M}^M \delta_{\Delta,\sigma}^{(1)}(k\Delta x)W_{i,j+k} + G_{233} \sum_{k=-M}^M \delta_{\Delta,\sigma}^{(2)}(k\Delta x)W_{i+k,j} \\ = -\rho h \omega^2 V_{i,j}, \quad (43b) \end{aligned}$$

$$\begin{aligned}
 &G_{311}U_{i,j} + G_{312} \sum_{k=-M}^M \delta_{\Delta,\sigma}^{(1)}(k\Delta x)U_{i+k,j} \\
 &+ G_{321}V_{i,j} + G_{322} \sum_{k=-M}^M \delta_{\Delta,\sigma}^{(1)}(k\Delta x)V_{i,j+k} + G_{323} \sum_{k=-M}^M \delta_{\Delta,\sigma}^{(2)}(k\Delta x)V_{i+k,j} \\
 &+ G_{331}W_{i,j} + G_{332} \sum_{k=-M}^M \delta_{\Delta,\sigma}^{(1)}(k\Delta x)W_{i,j+k} + G_{333} \sum_{k=-M}^M \delta_{\Delta,\sigma}^{(2)}(k\Delta x)W_{i+k,j} \\
 &+ G_{334} \sum_{k=-M}^M \delta_{\Delta,\sigma}^{(3)}(k\Delta x)W_{i+k,j} + G_{335} \sum_{k=-M}^M \delta_{\Delta,\sigma}^{(4)}(k\Delta x)W_{i+k,j} \\
 &= -\rho h \omega^2 W_{i,j}, \quad (43c)
 \end{aligned}$$

where the  $\delta_{\alpha,\sigma}^{(n)}$  are the coefficients of the regularized Shannon kernel, listed in the Appendix. Thus, the governing equations are spatially discretized by using the DSC algorithm. The DSC form of the boundary conditions can be easily written. For the clamped edge, for example, given as

$$U_{i,j} = 0, \quad V_{i,j} = 0, \quad W_{i,j} = 0 \quad \text{and} \quad \sum_{k=-M}^M \delta_{\Delta,\sigma}^{(1)}(k\Delta x)W_{i+k,j} = 0. \quad (44)$$

Wei et al. [2002a] proposed a practical method to treatment of the boundary conditions for DSC. Zhao and Wei [2002] proposed a practical method to incorporate the boundary conditions. More recently, the iteratively matched boundary method has been applied [Zhao et al. 2005; Zhou et al. 2006] to impose the free boundary conditions for the solid mechanic problem.

By the DSC rule, the governing equations and the corresponding boundary conditions can be replaced by a system of simultaneously linear algebraic equations in terms of the displacements at all the sampling points. It is noted that for a well-posed problem the number of equations should be identical to the the number of unknowns. A treatment commonly used in the literature [Shu 1996b; Wu and Wu 2000; Civalek 2004] is applied in this study. The first two governing equations in (43) are applied at interior points ( $k = 2, 3, \dots, M - 1$ ) and third governing equation is applied at the interior points ( $k = 3, 4, \dots, M - 2$ ). By rearranging the DSC form of the governing equations, one has the assembled form of the resulting equations as

$$[[G_{dd}] \ [G_{db}]] \begin{Bmatrix} \{U_d\} \\ \{U_b\} \end{Bmatrix} - \Omega [[B_{dd}] \ [B_{db}]] \begin{Bmatrix} \{U_d\} \\ \{U_b\} \end{Bmatrix} \{0\} \quad (45)$$

where  $\{U_b\}$  represents the unknown boundary grid points values, whereas  $\{U_d\}$  represent the domain grid point unknowns. The subscript  $b$  represents the degree of freedom on the boundary and subscript  $d$  represents the degree of freedom on the domain. Substituting the DSC rule into the boundary conditions at the sampling points at two boundary points leads to

$$[[G_{bd}] \ [G_{bb}]] \begin{Bmatrix} \{U_d\} \\ \{U_b\} \end{Bmatrix} = \{0\} \quad (46)$$

After rewriting this as  $U_b = -G_{bb}^{-1}G_{bd}U_d$  and then substituting the resulting equation into (45), we obtain

$$GU = \Omega BU \quad (47)$$

where  $G = G_{dd} - G_{db}G_{bb}^{-1}G_{bd}$ ,  $B = B_{dd} - B_{db}G_{bb}^{-1}G_{bd}$ , and  $U$  is the displacement vector on the domain. In the above eigenvalue equation,  $\Omega$  is the nondimensional frequency parameter. In (47),  $G$  and  $B$  are the matrices derived from the governing equations described by (43) and the boundary conditions considered in (44).

#### 4. Numerical applications

This section presents some numerical results for the free vibration analysis of laminated conical shells. The utility and robustness of the proposed method is illustrated by a number of numerical examples in this section. In order to simplify the presentation, S and C represent simply supported, and clamped supports, respectively. Firstly, the convergence of DSC results is studied. To check whether the purposed formulation and programming are correct, an isotropic conical shell is analysed first. The numerical results are given by the dimensionless frequency parameter  $\Omega$ , defined by

$$\Omega = R_2 \sqrt{\frac{\rho h}{A_{11}}} \omega$$

where  $\omega$  is referred to as the frequency parameter. The obtained results by DSC are listed in Table 1. This table shows the convergence of computed frequency parameters  $\Omega$  for an isotropic conical shell with  $\theta = 60^\circ$ ,  $L \sin \theta / R_2 = 0.75$  and circumferential wave number  $n = 0$ . The table also shows results given in [Irie et al. 1984; Tong 1993a; Shu 1996a]. To examine the influence of bandwidth on the accuracy, we choose five values of  $N$  (8, 11, 16, 21, 32), with corresponding regularization parameters  $\sigma / \Delta = 1.73, 2.15, 2.46, 2.8$  and 3.2, and set  $M = N$  with  $r$  optimally selected. From Table 1, it is seen that the convergence of DSC results is very good. In comparison with the results in [Irie et al. 1984], DSC results using 16 uniform grid points are very accurate. When the number of grid points is larger than 16, the DSC results are grid-independent. The fundamental frequency param-

	$L \sin \alpha / R_2 = 0.25$				
	$\alpha = 15^\circ$	$\alpha = 30^\circ$	$\alpha = 45^\circ$	$\alpha = 60^\circ$	$\alpha = 75^\circ$
$N = 8$	0.8983	0.9058	0.8204	0.7704	0.6629
$N = 11$	0.8355	0.8901	0.8151	0.7556	0.6447
$N = 16$	0.7851	0.8935	0.8043	0.7357	0.6228
$N = 21$	0.7856	0.8941	0.8047	0.7361	0.6234
$N = 32$	0.7856	0.8941	0.8047	0.7361	0.6234
[Irie et al. 1984]	—	0.8938	0.8041	0.7353	—
[Tong 1993b]	—	0.8938	0.8041	0.7353	—
[Shu and Du 1997]	—	—	—	0.7366	—

**Table 1.** Frequency parameters of C-S conical shells;  $\nu = 0.3$ ,  $h/R_2 = 0.01$ ,  $n = 0$ .

eters  $\Omega$  for an antisymmetric cross-ply laminated circular cylindrical shell with the S-C boundary condition are shown in Table 2. This table shows the fundamental frequency parameters based on classical shell theory (CST) [Shu and Du 1997] and the present DSC formulation. The results in Wu and Lee [2001], obtained using the differential quadrature method (DQM), are also listed for comparison. Note that

h/R	L/R	Present DST results		CST [Shu and Du 1997]		DQM [Wu and Lee 2001] for $N = 11$	
		max.cplg	no cplg	max.cplg	no cplg	max.cplg	no cplg
		$N_L = 2$	$N_L = \infty$	$N_L = 2$	$N_L = \infty$	$N_L = 2$	$N_L = \infty$
0.01	1	0.6585	0.7729	0.6440	0.8044	0.6725	0.8003
	2	0.3802	0.4463	0.3750	0.4545	0.3742	0.4534
	5	0.1849	0.2186	0.1858	0.2193	0.1852	0.2187
	10	0.1014	0.1195	0.1030	0.1223	0.1027	0.1217
	20	0.0477	0.0628	0.0496	0.0641	0.0494	0.0639
0.05	1	1.1406	1.4803	1.3201	1.8327	1.2820	1.6531
	2	0.6228	0.7474	0.6518	0.8146	0.6432	0.7975
	5	0.2785	0.3502	0.2886	0.3615	0.2876	0.3562
	10	0.1663	0.1956	0.1745	0.2021	0.1733	0.2015
	20	0.0771	0.0787	0.0875	0.0886	0.0870	0.0881

**Table 2.** Fundamental frequency parameters of an antisymmetric cross-ply laminated circular cylindrical shell with the S-C boundary condition ( $\nu = 0.3$ ,  $h/R_2 = 0.01$ ).

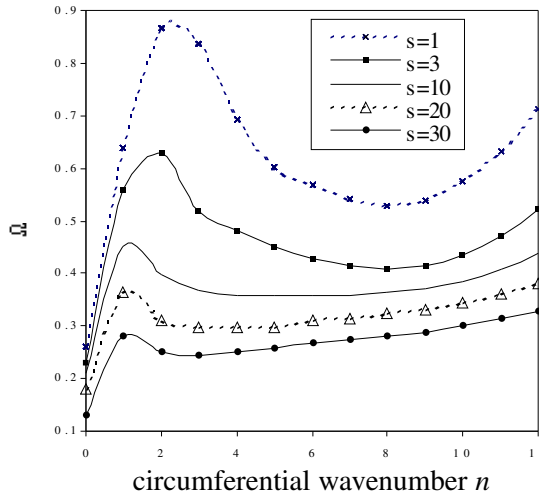


**Figure 2.** Effect of  $s = E_x/E_\theta$  ratio on frequency with the S-S boundary condition for cone angle  $15^\circ$  ( $L \sin \alpha/R_2 = 0.25$ ;  $h/R_2 = 0.01$ .)

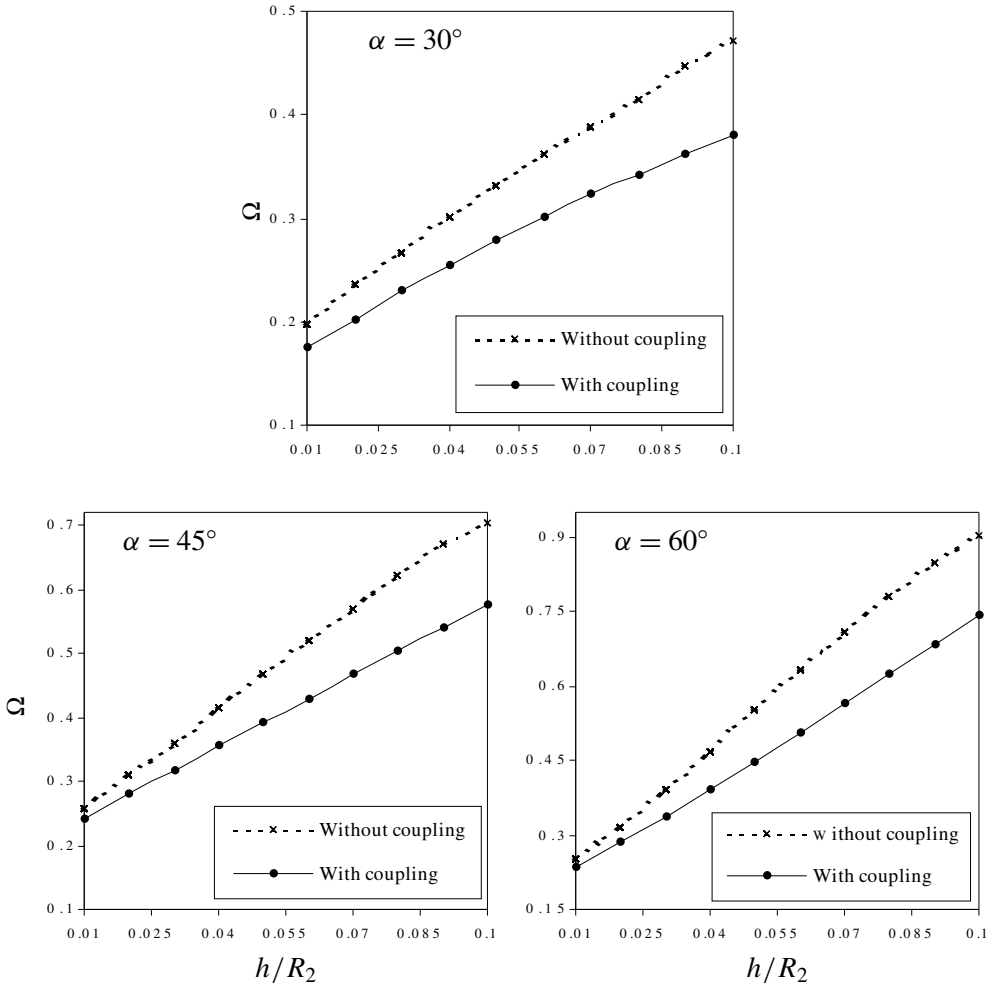
$N = 11$  is sufficient to obtain accurate results. The present numerical solutions are in close agreement with the DQM and CST solutions available in the literature. We also see from Table 2 that the results of two layers ( $N_L = 2$ ) are always less than that of infinite layers ( $N_L = \infty$ ). This suggests that the fundamental frequency parameters decrease as the coupling rigidity terms increase.

Figure 2 shows the frequency parameters of clamped and simply supported orthotropic conical shells for  $\mu_{x\phi} = 0.3$ ,  $s = E_x/E_\theta$ ,  $E_x = 2.1 \times 10^6$  and  $G_{x\theta} = 807692$ . The effects of the ratio  $s$  on the values of  $\Omega$  for  $\alpha = 15^\circ$  are displayed. Note that the values of  $\Omega$  decrease when the ratio  $s$  increases. The variation is marginal for larger values of  $s$ , irrespective of cone angles. In general,  $\Omega$  increases considerably with circumferential wave number for larger values of  $s$  ( $s > 10$ ).

To examine the influence of  $h/R_2$  on the frequency characteristics for S-S boundary conditions, we plot in Figure 3 the dependence for three different cone angles  $\alpha$  ( $30^\circ$ ,  $45^\circ$ ,  $60^\circ$ ). With the increase of ratio  $h/R_2$ , the frequency parameter  $\Omega$  increases rapidly. Generally, decreasing the cone angle also decreases the frequency parameter  $\Omega$ .

Figure 4 shows the effect of  $h/R_2$  on the frequency, and suggests that the frequency parameter increases uniformly with the ratio  $h/R_2$ . The C-C conical shell has the highest frequency parameter, followed by C-S and S-C. The S-S conical shell has the lowest frequency parameter.

For the ratio  $L/R_2 = 0.5$ , Figure 5 highlights the influence of the geometric ratio  $h/R_2$  on the frequency parameter  $\Omega$ , for four different cone angles  $\alpha$ . We see



**Figure 3.** Variation of frequency  $\Omega$  with geometric ratio  $h/R_2$  for S-S conical shell, for various values of  $\alpha$ .

that this influence is significant, that increasing  $\alpha$  always increases  $\Omega$ , and that the influence of the boundary condition on  $\Omega$  with  $h/R_2$  is significant.

Figure 6 shows the frequency parameters of (0/90/0) laminated conical shells with S-S boundary conditions for the ratio  $L/R_1 = 5$ . The layer material properties are  $\nu_{12} = 0.25$ ,  $\nu_{22} = 0.25$ ,  $E_{11}/E_{22} = 25$ ,  $G_{12}/E_{22} = 0.5$ ,  $G_{22}/E_{22} = 0.2$ . These figures show the effects of the ratio  $h/R_1$  on the values of  $\Omega$  for two types of cone angles,  $\alpha = 30^\circ$  and  $\alpha = 60^\circ$ . The variation is only marginal for larger values of  $n$ , irrespective of cone angles. For the cases under consideration, axisymmetric frequencies ( $n = 0$ ) are not the lowest frequencies. The lowest frequencies occur for a higher value of  $n$ .

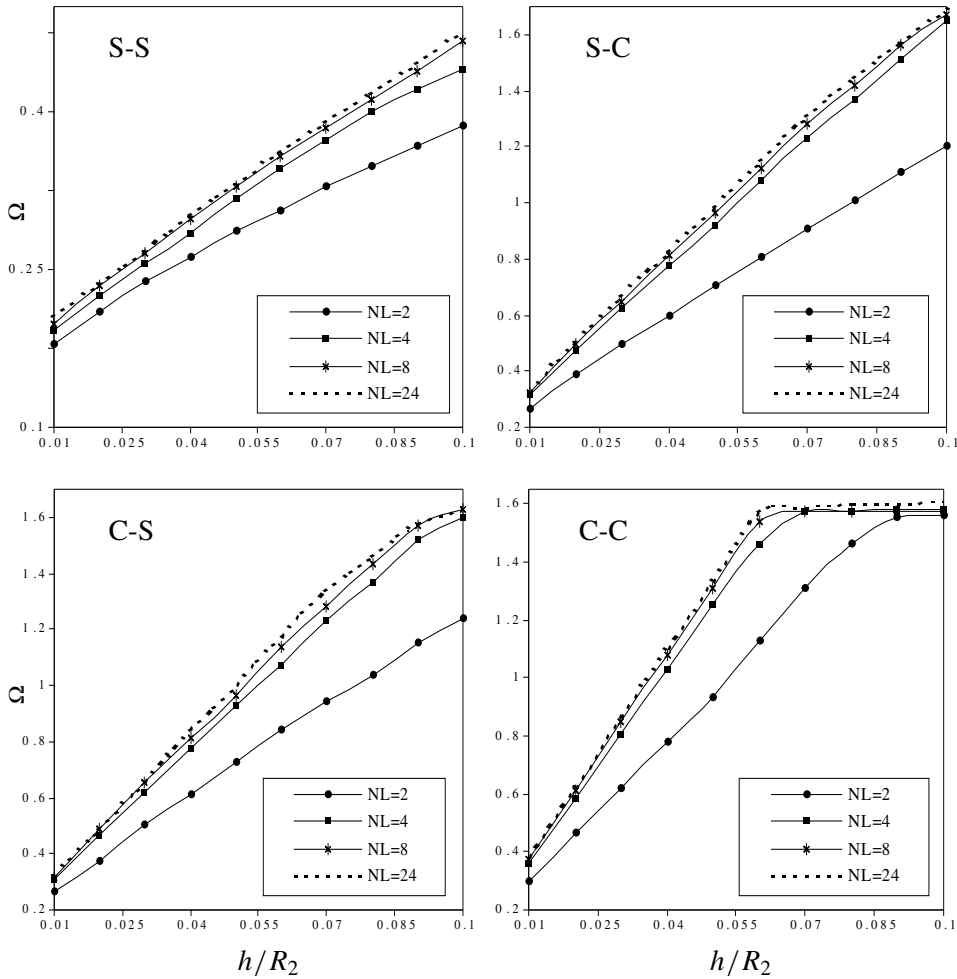


**Figure 4.** Variation of frequency  $\Omega$  with geometric ratio  $h/R_2$  for various conical shells ( $\alpha = 30^\circ$ ,  $L \sin \alpha/R_2 = 0.25$ ).

## 5. Conclusions

In conjunction with the method of DSC, the free vibration of orthotropic laminated conical shells is presented. Convergence tests are performed to validate the proposed approach for handling various combinations of two types of boundary conditions. A number of numerical examples are considered to explore the usefulness and test the accuracy of the present method. Accurate solutions have been presented for the frequencies of orthotropic laminated conical shells. The cone angle  $\alpha$  and the  $L \sin \alpha/R_2$  ratio has been found to have significant influence on the frequency parameters of the conical shell. The approach has been validated by convergence studies and comparisons with existing results in the literature.

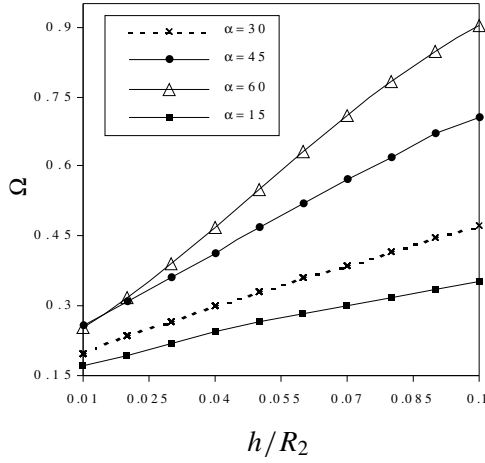


**Figure 5.** Variation of frequency  $\Omega$  with geometric ratio  $h/R_2$  for various cone angles of S-S conical shell ( $L/R_2 = 0.5$ ;  $h/R_2 = 0.01$ ;  $\nu = 0.3$ ).

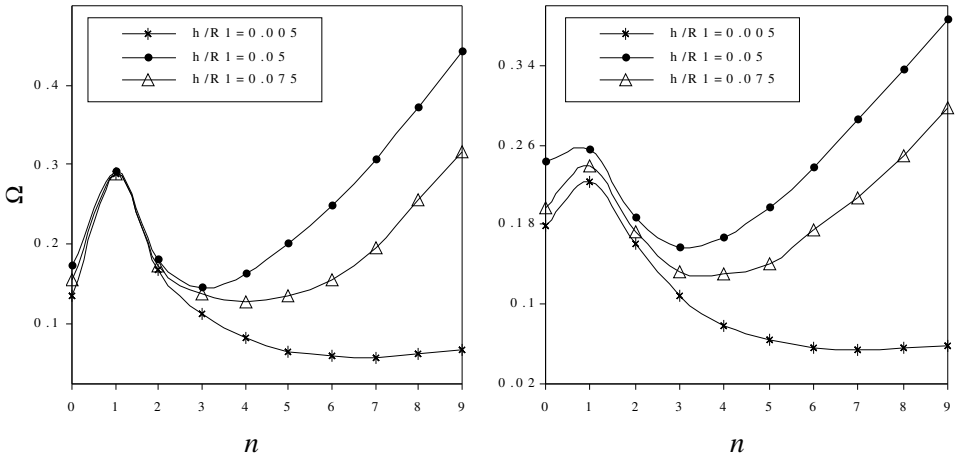


**Figure 6.** Variation of frequency  $\Omega$  with value of  $n$  for 0/90/0 laminated conical shells with S-S boundary conditions ( $L/R_1 = 5$ ). Left:  $\alpha = 30^\circ$ . Right:  $\alpha = 60^\circ$ .

### Appendix: The derivatives $\delta_{\Delta,\sigma}^{(n)}$

Here are the first four derivatives of the function  $\delta_{\Delta,\sigma}(x)$ , needed in Equations (43). For brevity, we set  $\xi := x - x_k$ ,  $s = \sin(\pi/\Delta)$ ,  $c = \cos(\pi/\Delta)$ .

$$\begin{aligned}\delta_{\pi/\Delta,\sigma}^{(1)}(x_m - x_k) &= e^{-\xi^2/2\sigma^2} \left( c - \frac{\Delta}{\pi} s \left( \frac{1}{\xi} + \frac{\xi}{\sigma^2} \right) \right), \\ \delta_{\pi/\Delta,\sigma}^{(2)}(x_m - x_k) &= e^{-\xi^2/2\sigma^2} \left( -\frac{\pi}{\Delta} s - \left( \frac{2}{\xi} + \frac{2\xi}{\sigma^2} \right) c + \frac{\Delta}{\pi} \left( \frac{2}{\xi^2} + \frac{1}{\sigma^2} + \frac{\xi^2}{\sigma^4} \right) s \right), \\ \delta_{\pi/\Delta,\sigma}^{(3)}(x_m - x_k) &= e^{-\xi^2/2\sigma^2} \left( -\frac{\pi^2}{\Delta^2} c + \frac{\pi}{\Delta} \left( \frac{3}{\xi} + \frac{3\xi}{\sigma^2} \right) s + \left( \frac{6}{\xi^2} + \frac{3}{\sigma^2} + \frac{3\xi^2}{\sigma^4} \right) c \right. \\ &\quad \left. - \frac{\Delta}{\pi} \left( \frac{6}{\xi^3} + \frac{3}{\xi\sigma^2} + \frac{\xi^3}{\sigma^4} \right) s \right), \\ \delta_{\pi/\Delta,\sigma}^{(4)}(x_m - x_k) &= e^{-\xi^2/2\sigma^2} \left( \frac{\pi^3}{\Delta^3} s + \frac{\pi^2}{\Delta^2} \left( \frac{4}{\xi} + \frac{4\xi}{\sigma^2} \right) c - \frac{\pi}{\Delta} \left( \frac{12}{\xi^2} + \frac{6}{\sigma^2} + \frac{6\xi^2}{\sigma^4} \right) s \right. \\ &\quad \left. - \left( \frac{24}{\xi^3} + \frac{12}{\xi\sigma^2} + \frac{4\xi^3}{\sigma^6} \right) c + \frac{\Delta}{\pi} \left( \frac{24}{\xi^4} + \frac{12}{\xi^2\sigma^2} + \frac{3}{\sigma^4} - \frac{2\xi^2}{\sigma^6} + \frac{\xi^4}{\sigma^8} \right) s \right).\end{aligned}$$

### Acknowledgements

The financial support of the Scientific Research Projects Unit of Akdeniz University is gratefully acknowledged.

### References

- [Bacon and Bert 1967] M. Bacon and C. W. Bert, “Unsymmetric free vibrations of orthotropic sandwich shells of revolution”, *AIAA J.* **5**:3 (1967), 413–417.
- [Chang 1981] C. H. Chang, “Vibration of conical shells”, *Shock Vib. Dig.* **13**:1 (1981), 9–17.
- [Civalek 1998] Ö. Civalek, “Finite-element analyses of plates and shells”, Firat University, Elazığ, 1998. In Turkish.
- [Civalek 2004] Ö. Civalek, *Geometrically non-linear static and dynamic analysis of plates and shells resting on elastic foundation by the method of polynomial differential quadrature (PDQ)*, Ph.D. thesis, Firat University, Elazığ, 2004. In Turkish.
- [Civalek 2005] Ö. Civalek, “Geometrically nonlinear dynamic analysis of doubly curved isotropic shells resting on elastic foundation by a combination of HDQ–FD methods”, *Int. J. Pressure Vessels Piping* **82**:6 (2005), 470–479.
- [Civalek and Ülker 2005] Ö. Civalek and M. Ülker, “HDQ–FD integrated methodology for nonlinear static and dynamic response of doubly curved shallow shells”, *Int. J. Struct. Engin. Mech.* **19**:5 (2005), 535–550.
- [Hua 2000] L. Hua, “Frequency characteristics of a rotating truncated circular layered conical shell”, *Compos. Struct.* **50**:1 (2000), 59–68.

- [Hua and Lam 2000] L. Hua and K. Y. Lam, "The generalized differential quadrature method for frequency analysis of a rotating conical shell with initial pressure", *Int. J. Numer. Meth. Eng.* **48**:12 (2000), 1703–1722.
- [Irie et al. 1982] T. Irie, G. Yamada, and Y. Kaneko, "Free vibration of a conical shell with variable thickness", *J. Sound Vib.* **82**:1 (1982), 83–94.
- [Irie et al. 1984] T. Irie, G. Yamada, and K. Tanaka, "Natural frequencies of truncated conical shells", *J. Sound Vib.* **92**:3 (1984), 447–453.
- [Kapania 1989] R. K. Kapania, "A review on the analysis of laminated shells", *J. Pressure Vessel Technol. (ASME)* **111** (1989), 88–96.
- [Lam and Hua 1997] K. Y. Lam and L. Hua, "Vibration analysis of a rotating truncated circular conical shell", *Int. J. Solids Struct.* **34**:17 (1997), 2183–2197.
- [Leissa 1973] A. W. Leissa, "Vibration of shells", NASA, 1973.
- [Liew and Lim 1994] K. M. Liew and C. W. Lim, "Vibratory characteristics of cantilevered rectangular shallow shells of variable thickness", *AIAA J.* **32**:2 (1994), 387–396.
- [Liew et al. 1995] K. M. Liew, M. K. Lim, C. W. Lim, D. B. Li, and Y. R. Zhang, "Effects of initial twist and thickness variation on the vibration behaviour of shallow conical shells", *J. Sound Vib.* **180**:2 (1995), 271–296.
- [Liew et al. 2005] K. M. Liew, T. Y. Ng, and X. Zhao, "Free vibration analysis of conical shells via the element-free kp-Ritz method", *J. Sound Vib.* **281**:3–5 (2005), 627–645.
- [Lim and Kitipornchai 1999] C. W. Lim and S. Kitipornchai, "Effects of subtended and vertex angles on the free vibration of open conical shell panels: a conical co-ordinate approach", *J. Sound Vib.* **219**:5 (1999), 813–835.
- [Lim and Liew 1995] C. W. Lim and K. M. Liew, "Vibratory behaviour of shallow conical shells by a global Ritz formulation", *Eng. Struct.* **17**:1 (1995), 63–70.
- [Lim et al. 1997] C. W. Lim, K. M. Liew, and S. Kitipornchai, "Free vibration of pretwisted, cantilevered composite shallow conical shells", *AIAA J.* **35**:2 (1997), 327–333.
- [Lim et al. 1998] C. W. Lim, K. M. Liew, and S. Kitipornchai, "Vibration of cantilevered laminated composite shallow conical shells", *Int. J. Solids Struct.* **35**:15 (1998), 1695–1707.
- [Lim et al. 2005a] C. W. Lim, Z. R. Li, and G. W. Wei, "DSC–Ritz method for high-mode frequency analysis of thick shallow shells", *Int. J. Numer. Meth. Eng.* **62**:2 (2005), 205–232.
- [Lim et al. 2005b] C. W. Lim, Z. R. Li, Y. Xiang, G. W. Wei, and C. Wang, "On the missing modes when using the exact frequency relationship between Kirchhoff and Mindlin plates", *Adv. Vib. Eng.* **4** (2005), 221–248.
- [Love 1888] A. E. H. Love, "On the small free vibrations and deformations of thin elastic shells", *Philos. T. Roy. Soc. A* **179A** (1888), 491–546.
- [Shu 1996a] C. Shu, "An efficient approach for free vibration analysis of conical shells", *Int. J. Mech. Sci.* **38**:8–9 (1996), 935–949.
- [Shu 1996b] C. Shu, "Free vibration analysis of composite laminated conical shells by generalized differential quadrature", *J. Sound Vib.* **194**:4 (1996), 587–604.
- [Shu and Du 1997] C. Shu and H. Du, "Free vibration analysis of laminated composite cylindrical shells by DQM", *Compos. B: Eng.* **28**:3 (1997), 267–274.
- [Siu and Bert 1970] C. C. Siu and C. W. Bert, "Free vibrational analysis of sandwich conical shells with free edges", *J. Acoust. Soc. Am.* **47**:3B (1970), 943–945.
- [Sivadas and Ganesan 1992] K. R. Sivadas and N. Ganesan, "Vibration analysis of thick composite clamped conical shells of varying thickness", *J. Sound Vib.* **152**:1 (1992), 27–37.

- [Soedel 1996] W. Soedel, *Vibrations of shells and plates*, 2nd ed., Marcel Dekker, New York, 1996.
- [Tong 1993a] L. Tong, “Free vibration of composite laminated conical shells”, *Int. J. Mech. Sci.* **35**:1 (1993), 47–61.
- [Tong 1993b] L. Tong, “Free vibration of orthotropic conical shells”, *Int. J. Eng. Sci.* **31**:5 (1993), 719–733.
- [Tong and Wang 1992] L. Tong and T. K. Wang, “Simple solutions for buckling of laminated conical shells”, *Int. J. Mech. Sci.* **34**:2 (1992), 93–111.
- [Wan et al. 2002] D. C. Wan, Y. C. Zhou, and G. W. Wei, “Numerical solution of incompressible flows by discrete singular convolution”, *Int. J. Numer. Meth. Fl.* **38**:8 (2002), 789–810.
- [Wei 1999] G. W. Wei, “Discrete singular convolution for the solution of the Fokker–Planck equation”, *J. Chem. Phys.* **110**:18 (1999), 8930–8942.
- [Wei 2001a] G. W. Wei, “A new algorithm for solving some mechanical problems”, *Comput. Methods Appl. Mech. Eng.* **190**:15–17 (2001), 2017–2030.
- [Wei 2001b] G. W. Wei, “Vibration analysis by discrete singular convolution”, *J. Sound Vib.* **244**:3 (2001), 535–553.
- [Wei et al. 2002a] G. W. Wei, Y. B. Zhao, and Y. Xiang, “Discrete singular convolution and its application to the analysis of plates with internal supports. Part 1: Theory and algorithm”, *Int. J. Numer. Meth. Eng.* **55**:8 (2002), 913–946.
- [Wei et al. 2002b] G. W. Wei, Y. B. Zhao, and Y. Xiang, “A novel approach for the analysis of high-frequency vibrations”, *J. Sound Vib.* **257**:2 (2002), 207–246.
- [Wu and Lee 2001] C. P. Wu and C. Y. Lee, “Differential quadrature solution for the free vibration analysis of laminated conical shells with variable stiffness”, *Int. J. Mech. Sci.* **43**:8 (2001), 1853–1869.
- [Wu and Wu 2000] C. P. Wu and C. H. Wu, “Asymptotic differential quadrature solutions for the free vibration of laminated conical shells”, *Comput. Mech.* **25**:4 (2000), 346–357.
- [Yang 1974] C. C. Yang, “On vibrations of orthotropic conical shells”, *J. Sound Vib.* **34** (1974), 552–555.
- [Zhao and Wei 2002] Y. B. Zhao and G. W. Wei, “DSC analysis of rectangular plates with non-uniform boundary conditions”, *J. Sound Vib.* **255**:2 (2002), 203–228.
- [Zhao et al. 2002] Y. B. Zhao, G. W. Wei, and Y. Xiang, “Discrete singular convolution for the prediction of high frequency vibration of plates”, *Int. J. Solids Struct.* **39**:1 (2002), 65–88.
- [Zhao et al. 2005] S. Zhao, G. W. Wei, and Y. Xiang, “DSC analysis of free-edged beams by an iteratively matched boundary method”, *J. Sound Vib.* **284**:1–2 (2005), 487–493.
- [Zhou et al. 2006] Y. C. Zhou, S. Zhao, M. Feig, and G. W. Wei, “High order matched interface and boundary method for elliptic equations with discontinuous coefficients and singular sources”, *J. Comput. Phys.* **213**:1 (2006), 1–30.

Received 29 Sep 2005. Revised 28 Nov 2005.

ÖMER CİVALEK: [civalek@yahoo.com](mailto:civalek@yahoo.com)

Akdeniz Üniversitesi, Mühendislik Fakültesi, İnşaat Mühendisliği Bölümü, 07200 Antalya, Türkiye